HHS Public Access

Author manuscript

Proc Am Control Conf. Author manuscript; available in PMC 2016 December 14.

Published in final edited form as:

Proc Am Control Conf. 2016 July ; 2016: 4793–4800. doi:10.1109/ACC.2016.7526112.

Decentralized Feedback Controllers for Exponential Stabilization of Hybrid Periodic Orbits: Application to Robotic Walking*

Kaveh Akbari Hamed[1] and **Robert D. Gregg**[2]

[1]Department of Mechanical Engineering, San Diego State University, San Diego, CA 92182-1323 USA

[2]Department of Mechanical Engineering, University of Texas at Dallas, Richardson, TX 75080-3021 USA

Abstract

This paper presents a systematic algorithm to design time-invariant decentralized feedback controllers to exponentially stabilize periodic orbits for a class of hybrid dynamical systems arising from bipedal walking. The algorithm assumes a class of parameterized and nonlinear decentralized feedback controllers which coordinate lower-dimensional hybrid subsystems based on a common phasing variable. The exponential stabilization problem is translated into an iterative sequence of optimization problems involving bilinear and linear matrix inequalities, which can be easily solved with available software packages. A set of sufficient conditions for the convergence of the iterative algorithm to a stabilizing decentralized feedback control solution is presented. The power of the algorithm is demonstrated by designing a set of local nonlinear controllers that cooperatively produce stable walking for a 3D autonomous biped with 9 degrees of freedom, 3 degrees of underactuation, and a decentralization scheme motivated by amputee locomotion with a transpelvic prosthetic leg.

I. INTRODUCTION

The objective of this paper is to present a systematic algorithm to design *decentralized* feedback controllers that coordinate lower-dimensional subsystems to asymptotically stabilize periodic orbits for hybrid dynamical systems. The algorithm considers a class of parameterized and nonlinear decentralized feedback controllers. It provides cooperation among subsystems of complex 3D walking models in the presence of underactuation.

Previous work on bipedal walking made use of multilevel *centralized* nonlinear feedback control architectures to stabilize periodic orbits [1]–[11]. However, human locomotion may employ a decentralized control scheme relying heavily on local feedback loops [12], [13]. Centralized control schemes designed for bipedal robots also *cannot* be easily transferred to powered prosthetic legs, which act as decentralized subsystems. In particular, centralized

*The work of K. Akbari Hamed was partially supported by the Center for Sensorimotor Neural Engineering (CSNE) that is an NSF Engineering Research Center. The work of R.D. Gregg was supported by the National Institute of Child Health & Human Development of the NIH under Award Number DP2HD080349. The content is solely the responsibility of the authors and does not necessarily represent the official views of the NIH. R. D. Gregg holds a Career Award at the Scientific Interface from the Burroughs Welcome Fund.

feedback architectures would require state measurements from both the prosthesis and human body, i.e., two interconnected subsystems. It would not be clinically feasible for users of prosthetic legs to wear sensors at all their intact joints. Although powered prosthetic legs already use decentralized feedback controllers related to joint impedance [14], this *linear* control method requires different control parameters at different time periods to handle the nonlinear dynamics of the gait cycle. The resulting “finite state machine” requires clinicians to spend significant amounts of time tuning each controller to a patient [15] and risks instability when perturbations cause the wrong controller to be used at the wrong time [16]–[18]. The limitations of this sequential control method could possibly be addressed by the unifying *nonlinear* controllers used in dynamic walking robots. This underlines the importance of developing decentralized nonlinear feedback algorithms for stabilizing hybrid periodic orbits.

State-of-the-art decentralized controllers for large-scale systems pertain to the stabilization of *equilibrium points* for ordinary differential equations (ODEs) and *not* periodic orbits of hybrid dynamical systems [19]–[23]. The design of decentralized control schemes for hybrid dynamical models of bipedal robots is an extremely difficult problem. Significant complexity arises from the high dimensionality, strong interactions among subsystems, underactuation, and hybrid nature of these models. The most basic tool for analyzing the stability of periodic orbits of hybrid dynamical systems—the Poincaré return map [2], [22], [24]—must be estimated *numerically*, which further complicates the design of decentralized controllers.

The contribution of this paper is to present a systematic algorithm to design a class of decentralized nonlinear feedback controllers that asymptotically stabilize periodic orbits for the hybrid models of bipedal walking. The proposed algorithm assumes a finite set of parameterized local controllers so that (1) they are coordinated based on a common *phasing variable*, (2) a periodic orbit is induced, and (3) the orbit is invariant under the choice of controller parameters. These assumptions are satisfied for several classes of decentralized feedback controllers including virtual constraints [3]. We investigate nonlinear stability tools for hybrid systems to formulate the problem of designing decentralized nonlinear controllers as an iterative sequence of optimization problems involving Bilinear and Linear Matrix Inequalities (BMIs and LMIs). By design these optimization problems can be solved easily with available software packages. This paper also presents sufficient conditions on the Poincaré map to guarantee the convergence of the iterative BMI algorithm at a finite number of iterations. We previously applied a BMI algorithm for the systematic design of centralized feedback controllers in [25]–[27], whereas this paper presents a BMI framework for designing decentralized controllers. A class of novel decentralized controllers is first developed and then the BMI algorithm is improved for tuning the local controllers. Finally to demonstrate the power of the algorithm, we control the walking gait of a 3D autonomous robot with 9 degrees of freedom (DOFs) and 6 actuators, choosing a two-part decentralization scheme corresponding to a transpelvic (hip disarticulated) amputee walking with a robotic prosthetic leg. A byproduct of this work is the first known control strategy for a powered 3-DOF transpelvic prosthetic leg.

II. HYBRID MODEL OF WALKING

We consider hybrid dynamical systems with one continuous-time phase as follows

$$\sum: \begin{cases} \dot{x} = f(x) + g(x)\,u, & x^- \notin \mathscr{S} \\ x^+ = \Delta(x^-), & x^- \in \mathscr{S}, \end{cases} \quad (1)$$

where $x \in \mathscr{X}$ denotes the state variables and $\mathscr{X} \subset \mathbb{R}^n$ represents the state manifold. The continuous-time portion of the hybrid system is given by the ODE $\dot{x} = f(x)+g(x)u$, in which $u \in \mathscr{U}$ denotes the continuous-time control inputs and $\mathscr{U} \subset \mathbb{R}^m$ represents a set of admissible control inputs. The vector field $f: \mathscr{X} \to T\mathscr{X}$ and columns of g are assumed to be smooth (i.e., C^∞). The discrete-time portion of the hybrid system is given by the instantaneous *reset map* $x^+ = \Delta(x^-)$, where $\Delta : \mathscr{X} \to \mathscr{X}$ is C^∞ and $x^-(t) := \lim_{\tau \nearrow t} x(\tau)$ and $x^+(t) := \lim_{\tau \searrow t} x(\tau)$ represent the left and right limits of the state trajectory $x(t)$, respectively. The *switching manifold* $\mathscr{S}$ is then represented by $\mathscr{S} := \{x \in \mathscr{X} \,|\, s(x) = 0 \text{ and } \sigma(x) < 0\}$, where $s : \mathscr{X} \to \mathbb{R}$ is a C^∞ *switching function* which satisfies $\frac{\partial s}{\partial x}(x) \neq 0$ for all $x \in \mathscr{S}$. Finally, $\sigma: \mathscr{X} \to \mathbb{R}$ is assumed to be C^∞.

A. Hybrid Interconnected Subsystems

Throughout this paper, we shall assume that the hybrid model of (1) is composed of two *interconnected subsystems* Σ_1 and Σ_2 in which the *local state variables* and *local inputs* of the i-th subsystem are represented by $x_i \in \mathscr{X}_i \subset \mathbb{R}^{n_i}$ and $u_i \in \mathscr{U}_i \subset \mathbb{R}^{m_i}$, respectively, where the subscript $i \in \{1, 2\}$ denotes the subsystem number. Our motivation comes from biomimetic control of powered prostheses for which the typical model may consist of two subsystems including the "human" body and "prosthetic" part (see Fig. 1). The *global state variables* and *global inputs* of (1) are then assumed to be decomposed as $x = (x_1^\top, x_2^\top)^\top$ and $u = (u_1^\top, u_2^\top)^\top$ which result in $\mathscr{X} = \mathscr{X}_1 \times \mathscr{X}_2$ and $\mathscr{U} = \mathscr{U}_1 \times \mathscr{U}_2$.

We shall assume that there is a desired period-one orbit for the hybrid model of (1) which is transversal to the switching manifold $\mathscr{S}$. To make this notion more precise, we present the following assumption.

Assumption 1 (Transversal Period-one Orbit)—There exists a bounded scalar $T^\star > 0$ (referred to as the *fundamental period*), smooth *nominal local control inputs* $u_i^\star : [0, T^\star] \to \mathscr{U}_i$ for $i \in \{1, 2\}$, and a unique *nominal global state solution* $\varphi^\star(t)$ which satisfy the ODE of the continuous-time portion and *periodicity condition* as follows

$$\begin{array}{ll} \dot{\varphi}^\star(t) & = f(\varphi^\star(t)) + g(\varphi^\star(t))\, u^\star(t), \quad 0 \le t \le T^\star \\ \varphi^\star(0) & = \Delta(\varphi^\star(T^\star)) \\ \varphi^\star(t) & \notin \mathscr{S}, \quad 0 \le t < T^\star \quad \text{and} \quad \varphi^\star(T^\star) \in \mathscr{S}, \end{array}$$

where $u^\star(t) := (u_1^{\star\top}(t), u_2^{\star\top}(t))^\top$. Furthermore, the *period-one orbit* $\mathcal{O} := \{x = \varphi^\star(t) \mid 0 \le t < T^\star\}$ is assumed to be *transversal* to the switching manifold $\mathcal{S}$, i.e., $\dot{s}(\varphi^\star(T^\star)) \neq 0$.

Sections II-B and III will present the class of decentralized feedback controllers and the iterative BMI optimization algorithm to exponentially stabilize the desired periodic orbit $\mathcal{O}$, respectively.

B. Class of Decentralized Feedback Controllers

In our proposed decentralized feedback control structure, the local controllers are *parameterized* and *general nonlinear* feedback laws which have access to their own local measurements (i.e., local state variables x_i) as well as a *subset* of measurable global variables. *Global variables* are defined as quantities which depend on the global state variables. The global variable is said to be *measurable* for a subsystem if there are sensors to measure it along the solutions of that subsystem.

Assumption 2 (Measurable Global Variables)—It is assumed that the set of measurable global variables for sub-system Σ_i, $i \in \{1, 2\}$, can be written in the form of

$$\Psi_i(x) := \left(\psi_i^\top(x), \dot{\psi}_i^\top(x), \cdots, \psi_i^{(r-1)\top}(x)\right)^\top \in \mathbb{R}^{rv_i} \tag{2}$$

for some smooth measurable global variable $\psi_i(x) \in \mathbb{R}^{v_i}$ and some positive integers $v_i \ge 1$ and $r \ge 1$. We further assume that the control input u does *not* explicitly appear in the equations of $\psi_i(x), \dot{\psi}_i(x), \cdots$, and $\psi_i^{(r-1)}(x)$.

Example 1: For the case of powered prostheses in Fig. 1, without loss of generality let us assume that subsystems Σ_1 and Σ_2 represent the human and prosthetic leg parts, respectively. Suppose further that the human part has global orientation in its local state vector (assumed to come from the vestibular system), whereas the prosthetic part has only shape variables and therefore must utilize external inertial measurement units (IMUs) for measurements of orientation. Because orientation is implicitly included in the local state vector of the human part, its externally measured global variable set $\Psi_1(x)$ can be empty. We assume that the prosthetic orientation measurements come from two IMUs attached to the thigh links: one on the human thigh and the other on the prosthetic thigh. The set of measurable global variables $\Psi_2(x)$ for the prosthetic part Σ_2 can then be chosen as the Euler angles, i.e., $\psi_2(x)$, and their first-order time-derivatives, i.e., $\dot{\psi}_2(x)$, from these two IMUs (note that $r = 2$). The use of two IMUs by the prosthesis will later allow the BMI optimization to more easily find stable gaits. There is precedence for wearing sensors on the sound leg in prosthetic control methods [28], but we will attempt to eliminate the need for the second IMU in future work.

In order to coordinate the local controllers, we now consider a *common* set of measurable global variables for both subsystems Σ_1 and Σ_2 in the following assumption.

Assumption 3 (Measurable Phasing Variable)—There exists a smooth and scalar global variable $\theta(x)$, referred to as the *phasing variable*, which satisfies the following conditions:

1. $\theta(x)$ is strictly monotonic (i.e., strictly increasing or decreasing) along the periodic orbit $\mathcal{O}$;
2. the control input u does *not* explicitly appear in the equations of $\theta(x)$, $\dot{\theta}(x)$, ⋯, and $\theta^{(r-1)}(x)$; and
3. the sequence of θ and its time-derivatives up to the order $(r-1)$, i.e.,

$$\Theta(x) := \left(\theta(x), \dot{\theta}(x), \cdots, \theta^{(r-1)}(x)\right)^{\top} \in \mathbb{R}^r$$

are measurable global variables for both subsystems Σ_1 and Σ_2.

From Item 1 of Assumption 3, the phasing variable can replace time, which is a key to obtaining time-invariant controllers that realize asymptotic orbital stability of the periodic orbit $\mathcal{O}$. Item 2 states that the relative degree of $\theta(x)$ and $\psi_i(x)$ for $i \in \{1, 2\}$ with respect to the control input u are the *same* and equal to r. Our motivation for this assumption will be clarified in local output functions (7). For mechanical systems, the phasing variable is usually taken as a holonomic quantity and hence, $r = 2$. Item 3 of Assumption 3 is not restrictive for models of bipedal walking. In particular, one can define a proper phasing variable based on the absolute stance hip angle in the sagittal plane. This angle θ and its first-order time-derivative $\dot{\theta}$ may be measured for Σ_2 by the IMUs attached to the thigh links in Example 1. It is further reasonable to assume that this angle is available to the human through proprioception of the residual thigh.

Now we propose a class of parameterized local feedback controllers as follows

$$u_i = \Gamma_i(x_i, \Theta(x), \Psi_i(x), \xi_i), \quad i = 1, 2, \tag{3}$$

where $\xi_i \in \Xi_i \subset \mathbb{R}^{p_i}$ denotes the *parameters of the local controller i* to be determined. Here, $\Gamma_i : \mathcal{X}_i \times \mathbb{R}^r \times \mathbb{R}^{rv_i} \times \Xi_i \to \mathcal{U}_i$ is a general smooth function of local state variables x_i, measurable phasing variable and its time- derivatives $\Theta(x)$, measurable global variables $\Psi_i(x)$ for the subsystem Σ_i, and local parameters ξ_i. We remark that the local controllers of (3) depend on two different sets of measurable global variables. The first set is common between Σ_1 and Σ_2 and includes $\Theta(x)$, consisting of the phasing variable and its time-derivatives, to *coordinate* the local controllers. In particular, the phasing variable represents the progress of the system (e.g., robot) on the periodic orbit (e.g., gait). The second set includes the individual measurable global variables $\Psi_i(x)$ to *improve the stability* of the periodic orbit $\mathcal{O}$. For instance in Example 1, the prosthetic leg controller may improve the frontal stability by having access to the roll angles from the IMUs attached to the thigh links.

Remark 1: In the case of amputee locomotion in Example 1, mathematical models for the local controller of the human part are not known. However for the purpose of this paper, we assume that the human local controller can be modeled as a *phase-dependent* nonlinear feedback law in a similar manner to [18]. Evidence suggests that phase-dependent models reasonably predict human joint behavior even across perturbations [13]. Since the human part controller does not have access to the external IMUs attached to both thighs ($\Psi_1 = \varnothing$ but orientation is implicitly included in x_1), it is better to show the local controllers of (3) as follows:

$$u_1 = \Gamma_1(x_1, \Theta(x), \xi_1) \quad (4)$$

$$u_2 = \Gamma_2(x_2, \Theta(x), \Psi_2(x), \xi_2). \quad (5)$$

To have a unified notation, however, we make use of (3) for the rest of the paper. We remark that the objective of this paper is to show that the local feedback control structure of (4) and (5) can yield asymptotically stable 3D walking gaits.

C. Closed-Loop Hybrid Model

By employing the local feedback laws of (3), the parameterized closed-loop hybrid model becomes

$$\sum_{\xi}^{\mathrm{cl}}: \begin{cases} \dot{x} = f^{\mathrm{cl}}(x, \xi), & x^- \notin \mathscr{S} \\ x^+ = \Delta(x^-, \xi), & x^- \in \mathscr{S}, \end{cases} \quad (6)$$

where $\xi := (\xi_1^\top, \xi_2^\top)^\top \in \Xi \subset \mathbb{R}^p$, $\Xi := \Xi_1 \times \Xi_2$ denotes the *set of admissible parameters; p* := $p_1 + p_2$, $f^{\mathrm{cl}}(x, \xi) := f(x) + g(x)\Gamma(x, \xi)$, and $\Gamma := (\Gamma_1^\top, \Gamma_2^\top)^\top$. The unique solution of the parameterized ODE $\dot{x} = f^{\mathrm{cl}}(x, \xi)$ with the initial condition $x(0) = x_0$ is denoted by $\varphi(t, x_0, \xi)$ for all $t \geq 0$ in the maximal interval of existence. The *time-to-reset* function, $T: \mathscr{X} \times \Xi \to \mathbb{R}_{>0}$, is then defined as the first time at which the ODE solution intersects the switching manifold $\mathscr{S}$, i.e., $T(x_0, \xi) := \inf\{t > 0 \mid \varphi(t, x_0, \xi) \in \mathscr{S}\}$.

Remark 2: In the closed-loop hybrid model of (6), the reset map Δ is also parameterized by ξ. Our motivation for this is to extend the iterative BMI algorithm for hybrid systems with multiple continuous-time phases. In particular, for these systems, the reset map can be expressed as a composition of the flows for the remaining continuous- and discrete-time phases. Consequently, Δ includes the parameters of the controllers employed during other continuous-time phases.

D. Invariant Periodic Orbit Assumption

Throughout this paper, we shall assume that the local feedback laws of (3) satisfy the *invariance* assumption. The invariance assumption states the periodic orbit $\mathcal{O}$ is invariant under the choice of the controller parameters $\xi=(\xi_1^\top,\xi_2^\top)^\top \in \Xi$. This helps us to preserve the orbit while tuning the parameters to improve its stability behavior. This assumption becomes more clear in the following assumption.

Assumption 4 (Invariant Periodic Orbit)—The closed-loop hybrid model (6) satisfies the following invariance conditions: 1) $\frac{\partial f^{\mathrm{cl}}}{\partial \xi}(x,\xi)=0$ for all $(x, \xi) \in \bar{\mathcal{O}} \times \Xi$, and 2) $\frac{\partial \Delta}{\partial \xi}(x^\star,\xi)=0$ for all $\xi \in \Xi$, where $\bar{\mathcal{O}}$ denotes the set closure of $\mathcal{O}$ and $\{x^\star\} := \bar{\mathcal{O}} \cap \mathcal{S}$.

To clarify the idea, we now present a family of the proposed decentralized controllers in (3) which satisfies the invariance assumption.

Local Output Zeroing Controllers—This family of local controllers is developed based on the *output regulation problem* for local subsystems Σ_i, $i \in \{1, 2\}$. We define a set of *parameterized local outputs* as follows

$$y_i\left(x_i,\Theta(x),\Psi_i(x,\xi_i)\right)=H_i(\xi_i)\left(x_i-x_{\mathrm{d},i}\left(\theta\right)\right)+\hat{H}_i(\xi_i)\left(\psi_i-\psi_{\mathrm{d},i}\left(\theta\right)\right), \quad (7)$$

where $\dim(y_i) = \dim(u_i) = m_i$, and $H_i(\xi_i) \in \mathbb{R}^{m_i \times n_i}$ and $\hat{H}_i(\xi_i) \in \mathbb{R}^{m_i \times v_i}$ are *local output matrices*, to be determined, which are parameterized by ξ_i. In addition, $x_{\mathrm{d},i}(\theta)$ and $\psi_{\mathrm{d},i}(\theta)$ represent the desired evolutions of the local state variables x_i and measurable global variables ψ_i on the periodic orbit $\mathcal{O}$, respectively, in terms of the phasing variable θ. According to the construction procedure, the local outputs (7) vanish on the desired orbit $\mathcal{O}$. Furthermore, we assume that r is the relative degree of the local output y_i with respect to the local input u_i. The family of local output zeroing controllers can then be chosen as[1]

$$\Gamma_i\left(x_i,\Theta(x),\Psi_i(x),\xi_i\right)=u_i^\star(\theta)-D_i^{-1}(x_i,\xi_i)\left(\sum_{j=0}^{r-1}k_j y_i^{(j)}\right),$$

where the term $u_i^\star(\theta)$ denotes the nominal local inputs of Assumption 1, regressed in terms of the phasing variable θ to preserve the periodic orbit $\mathcal{O}$ for the full-order model, $D_i(x_i, \xi_i)$ represents a smooth *local (lower-dimensional) decoupling matrix*[2], and the coefficients k_j for $j = 0, 1, \cdots, r-1$ are chosen such that the polynomial $\lambda^r + k_{r-1}\lambda^{r-1} + \cdots + k_0$ becomes Hurwitz. We remark that this family of local controllers is a decentralized approximation of centralized I/O linearizing controllers. In addition, it can be easily shown that

[1]We remark that $y_i^{(j)}$ is a function of $(\theta, \dot{\theta}, \ldots, \theta^{(j)})$ and $(\psi, \dot{\psi}_i, \ldots, \psi_i^{(j)})$ for all $j = 0, 1, \cdots, r-1$. This underlines the importance of having $\Theta(x)$ and $\Psi_i(x)$ measurable in Assumptions 2 and 3.

[2]It is assumed that $D_i(x_i, \xi_i)$ for $i \in \{1, 2\}$ is invertible on $\bar{\mathcal{O}} \times \Xi$ for some $\Xi \subset \mathbb{R}^p$.

$\frac{\partial f^{\mathrm{cl}}}{\partial \xi}(x,\xi)=g(x)\frac{\partial \Gamma}{\partial \xi}(x,\xi)=0$ for all $(x, \xi) \in \bar{\mathcal{O}} \times \Xi$, and hence, the invariance assumption is satisfied. For the case of Example 1 as stated in Remark 1, we choose $\hat{H}_1 = 0$ (or $\Psi_1 = \varnothing$) to have $u_1 = \Gamma_1(x_1, \Theta(x), \xi_1)$.

E. Poincaré Map and Exponential Stabilization

In order to exponentially stabilize the periodic orbit $\mathcal{O}$ for the closed-loop system (6), we define the *parameterized Poincaré map* as $P: \mathcal{X} \times \Xi \to \mathcal{X}$ by $P(x, \xi) := \varphi(T(\Delta(x, \xi), \xi), \Delta(x, \xi), \xi)$. This map describes the evolution of the closed-loop hybrid system (6) on the *Poincaré section* $\mathcal{S}$ according to the discrete-time system

$$x[k+1]=P(x[k],\xi), \quad k=0,1,2,\cdots. \tag{8}$$

From the invariance assumption, $x^\star$ is an *invariant fixed point* for the Poincaré map, that is $P(x^\star, \xi) = x^\star$ for all $\xi \in \Xi$. Linearization of (8) around the invariant fixed point $x^\star$ then results in

$$\delta x[k+1]=A(\xi)\,\delta x[k], \quad k=0,1,2,\cdots, \tag{9}$$

where $\delta x[k] := x[k] - x^\star$ and $A(\xi):=\frac{\partial P}{\partial x}(x^\star,\xi)$. Next we are interested in the following problem.

Problem 1 (Exponential Stabilization)—The problem of exponential stabilization of the periodic orbit $\mathcal{O}$ for the closed-loop hybrid system (6) consists of finding the parameter vector ξ such that the Jacobian matrix $A(\xi)$ becomes Hurwitz.

III. ITERATIVE BMI ALGORITHM

This section creates a systematic numerical algorithm to overcome specific difficulties arising from the lack of a closed-form expression for the Poincaré map, high dimensionality, and underactuation in tuning the decentralized feedback controllers of Section II-B for the hybrid model of (1). The objective is to tune the parameters of the decentralized feedback control structure of (3), i.e., $\xi=(\xi_1^\top,\xi_2^\top)^\top$, such that the desired orbit $\mathcal{O}$ becomes exponentially stable. Our iterative algorithm designs a sequence of controller parameters $\{\xi^\ell\}$, where the superscript $\ell \in \{0, 1, \cdots\}$ represents the iteration number. The objective is then to converge to a set of parameters ξ^ℓ that solves Problem 1. In what follows, we present the steps of the algorithm.

A. Step 1: Sensitivity Analysis and BMI Optimization

During iteration number ℓ, based on the Taylor series expansion of the Jacobian matrix around ξ^ℓ, i.e.,

$$A(\xi^\ell+\Delta\xi) \approx A(\xi^\ell)+\overline{A}(\xi^\ell)(I \otimes \Delta\xi), \quad (10)$$

a *sensitivity analysis* is employed to translate Problem 1 into an approximate exponential stabilization problem which can be expressed in terms of BMIs. In (10), $\Delta\xi$ is an increment in controller parameters with a sufficiently small norm $\|\Delta\xi\|$, "$\otimes$" represents the Kronecker product, and $\bar{A}(\xi^\ell)$ is referred to as the *sensitivity of the Jacobian matrix with respect to* ξ. Effective numerical approaches to calculate the Jacobian matrix $A(\xi^\ell)$ as well as the sensitivity matrix $\bar{A}(\xi^\ell)$ have been developed in [25, Theorems 1 and 2]. Next we present the approximate stabilization problem.

Problem 2 (Approximate Exponential Stabilization)—The problem of approximate exponential stabilization consists of tuning/incrementing the controller parameters $\Delta\xi^\ell := \xi^{\ell+1} - \xi^\ell$ such that the first-order approximation of the Jacobian matrix, i.e.,

$$\hat{A}(\xi^\ell, \Delta\xi^\ell) := A(\xi^\ell)+\overline{A}(\xi^\ell)(I \otimes \Delta\xi^\ell) \quad (11)$$

becomes Hurwitz.

In this paper, we follow the BMI optimization approach of [25] to solve Problem 2. However unlike [25], we repeat this approach in an *iterative* manner to converge to a set of stabilizing parameters[3]. In particular, during each iteration, we set up the following optimization problem

$$\min_{W,\Delta\xi^\ell,\mu,\eta} \; -w\,\mu+\eta \quad (12)$$

$$\text{s. t.} \quad \begin{bmatrix} W & \hat{A}(\xi^\ell, \Delta\xi^\ell)\,W \\ \star & (1-\mu)\,W \end{bmatrix} > 0 \quad (13)$$

$$\begin{bmatrix} I & \Delta\xi^\ell \\ \star & \eta \end{bmatrix} > 0 \quad (14)$$

$$\mu > 0, \quad (15)$$

[3]We have observed that for decentralized control problems one need to apply the BMI algorithm iteratively to converge to a stabilizing solution.

in which $W = W^\top$ is a positive definite symmetric matrix, $\mu > 0$ is a scalar to tune the spectral radius of $\hat{A}$, and η is a dynamic upper bound on $\|\Delta\xi^\ell\|_2^2$ to have a good approximation based on the Taylor series expansion in (10)[4]. Finally, $w > 0$ is a weighting factor as a trade-off between increasing μ (i.e., decreasing the spectral radius of $\hat{A}$) and decreasing η in the cost function (12). We remark that (13) and (14) represent BMI and LMI constraints, respectively.

B. Step 2: Iteration

Let ($W^{\ell\star}$, $\Delta\xi^{\ell\star}$, $\mu^{\ell\star}$, $\eta^{\ell\star}$) represent a *local* minimum for the BMI optimization problem (12)–(15)[5]. If the requirements of Problem 1 are satisfied at

$$\xi^{\ell+1} = \xi^\ell + \Delta\xi^{\ell\star}, \quad (16)$$

the algorithm terminates. Otherwise, the algorithm continues by coming back to the step of the sensitivity analysis and BMI optimization around the updated parameter $\xi^{\ell+1}$. In case the BMI optimization is not feasible, then the search process is not successful and the algorithm terminates.

C. Sufficient Conditions for Convergence of the Algorithm

The objective of this section is to present a set of sufficient conditions under which the iterative algorithm stabilizes the periodic orbit $\mathcal{O}$ for the closed-loop hybrid model (6) at a finite number of iterations. The conditions are presented in terms of the Poincaré map and its first-, second-, and third-order derivatives. For this goal, we present a *non-smooth* optimization problem which is equivalent to the BMI optimization problem (12)–(15). It is important to remak that we will not solve the non-smooth optimization problem numerically during the iterative algorithm. However, we will make use of this equivalent problem for the proof of the convergence in Theorems 1 and 2.

Lemma 1—The BMI optimization problem (12)–(15) is equivalent to

$$\min_{\Delta\xi^\ell, \gamma} \frac{1}{2} w \gamma^2 + \frac{1}{2} \|\Delta\xi^\ell\|_2^2 \quad (17)$$

$$\text{s. t.} \quad \rho\left(\hat{A}(\xi^\ell, \Delta\xi^\ell)\right) < \gamma \quad (18)$$

[4]In particular, $V(\delta x) = \delta x^\top W^{-1} \delta x$ is a Lyapunov function for $\delta x[k+1] = \hat{A}(\xi^\ell, \Delta\xi^\ell)\, \delta x[k]$ and $\sqrt{1-\mu}$ represents an upper bound for the spectral radius of $\hat{A}(\xi^\ell, \Delta\xi^\ell)$.

[5]More details about the local solutions will be presented in Section IV-B.

$$\gamma<1, \quad (19)$$

where $\rho(.)$ represents the spectral radius.

Proof: See Appendix.

Let us consider the Jacobian matrix $A(\xi) \in \mathbb{R}^{n\times n}$. For later purposes, we define the vectorization of the real and approximate Jacobian matrices as $a(\xi) := \text{vec}(A(\xi)) \in \mathbb{R}^{n^2}$ and $\hat{a}(\xi, \Delta\xi) := \text{vec}(\hat{A}(\xi, \Delta\xi)) \in \mathbb{R}^{n^2}$, where "vec(.)" represents the matrix vectorization operator. For the scalar case, i.e., $n = 1$, one can present a closed-form expression for the global solution of the equivalent problem (17)–(19). This helps us to present a set of sufficient conditions to guarantee the convergence of the iterative algorithm to a stabilizing set of parameters at a finite number of iterations.

Theorem 1 (Convergence of Algorithm for n = 1)—Consider the $\mathscr{C}^\infty$ scalar function $a : \mathbb{R} \to \mathbb{R}$ and suppose that there is $\bar{\xi} \in \mathbb{R}$ such that $a(\bar{\xi}) = 0$. Let $\mathscr{B}$ represent a compact (closed and bounded) ball around $\bar{\xi}$ such that 1) $a'(\xi) \neq 0$ for all $\xi \in \mathscr{B}$, and 2)

$$\max_{\xi\in\mathscr{B}} \frac{|a(\xi)|}{w\,(a'(\xi))^2+1}<1, \quad (20)$$

where $a'(\xi)$ denotes the first-order derivatives of $a(\xi)$. Then, there are $\delta > 0$ and $N < \infty$ such that for all initial guesses $\xi^0 \in \mathscr{B}$ with the property $|\xi^0 - \bar{\xi}| < \delta$, the iterative algorithm stabilizes the origin for (9) at N iterations, that is, $|a(\xi^\ell)| < 1$ for all $\ell > N$.

Proof: See Appendix.

For the multi-dimensional case, i.e., $n > 1$, there is not a closed-form expression for the optimal solution of (17)–(19) or for that of (12)–(15) to investigate the convergence of the algorithm similar to that presented in Theorem 1. However from Lemma 1, one can still present an alternative set of sufficient conditions to guarantee the stability of the real Jacobian matrix during iteration $\ell + 1$ based on a *local* optimal solution obtained during iteration ℓ. For this purpose, let $\chi(z) := \det(zI - A)$ represent the characteristic equation of a given matrix A. Then $\rho(A) < \gamma$ is equivalent to the monic polynomial $\frac{1}{\gamma^n}\chi(\gamma z)=\det(zI-\frac{1}{\gamma}A)$ being Hurwitz. From Jury stability criterion, this is also equivalent to the existence of $n + 1$ smooth inequality constraints on (a, γ) with $\gamma \neq 0$ as follows:

$$F_\alpha(a,\gamma)<0, \quad \alpha=1,\cdots,n+1, \quad (21)$$

where $a := \text{vec}(A) \in \mathbb{R}^{n^2}$. This enables the following result.

Theorem 2 (Convergence of Algorithm for n > 1)—Assume that the BMI optimization problem (12)–(15) is feasible during iteration ℓ. Suppose further that $(\Delta\xi^{\ell\star}, \mu^{\ell\star})$ denotes a *local* optimal solution (*not* necessarily the global solution). Then there is $\varepsilon > 0$ such that if 1) $\|\Delta\xi^{\ell\star}\| < \varepsilon$, and 2) the conditions

$$\sum_{\beta=1}^{n^2} \frac{\partial F_\alpha}{\partial a_\beta}\left(a(\xi^\ell), \sqrt{1-\mu^{\ell\star}}\right) \frac{\partial^2 a_\beta}{\partial \xi^2}(\xi^\ell) \leq 0 \tag{22}$$

for $\alpha = 1, \cdots, n+1$ are satisfied, then the algorithm terminates at the iteration $\ell+1$, that is, $A(\xi^\ell + \Delta\xi^{\ell\star})$ becomes Hurwitz. Here $a_\beta(\xi)$ represents the β-th component of $a(\xi)$ and $\frac{\partial^2 a_\beta}{\partial \xi^2}(\xi)$ denotes the corresponding Hessian matrix.

Proof: See Appendix.

We remark that the inequality conditions (22) can be viewed as $n+1$ LMI conditions on n^2 Hessian matrices $\frac{\partial^2 a_\beta}{\partial \xi^2}(\xi^\ell)$ for $\beta = 1, \cdots, n^2$. Hence, one can interpret these conditions as convexity requirements on the elements of $a(\xi)$ at $\xi = \xi^\ell$.

IV. APPLICATION TO ROBOTIC WALKING

Virtual constrains are kinematic relations among the generalized coordinates enforced asymptotically by continuous-time feedback control [2], [3], [7], [16], [17], [25], [26], [29]–[33]. They are defined to coordinate the links of the bipedal robot within a stride. In this approach, holonomic output functions $y(x)$ define desired virtual constraints, i.e., $y \equiv 0$, that are typically enforced by centralized input-output (I/O) linearizing feedback laws during the continuous-time portion of the hybrid system. Virtual constraint controllers have been validated numerically and experimentally for stable 2D and 3D underactuated bipedal robots [8], [29], [30], [34], [35] as well as 2D powered prosthetic legs [16]–[18]. The stability of walking gaits in the virtual constraints approach depends on the choice of the output functions [25]. The application of virtual constraints to prosthetics presents some challenges not previously encountered in autonomous robots, because centralized virtual constraint controllers would require state feedback from the human body. To overcome this problem associated with human interaction, [16] has approximated virtual constraint controllers using local *high-gain PD controllers* in simulations of a 2D powered prosthetic leg, but safety concerns limited the experimental implementation to inaccurate low-gain controllers. The local output functions for the prosthetic subsystem were also defined based on *physical intuition*. A recent approach measures the human interaction forces for exact local virtual constraint control [18], but multi-axis force sensors that are light enough for prosthetic limbs are extremely expensive.

There is currently no algorithm to systematically design decentralized virtual constraints to induce stable walking in bipedal robots and powered prosthetic legs. The objective of this section is to employ the iterative BMI optimization to search for stabilizing local virtual

constraints. We remark that the BMI optimization takes into account the interactions among the subsystems while searching for the optimized virtual constraints, preventing the need to employ impractical high-gain local controllers or expensive force sensors to deal with interactions.

A. 3D Underactuated Bipedal Robot

We apply the iterative BMI algorithm to tune the local output matrices for a set of decentralized virtual constraints in the form of (7) to exponentially stabilize the walking gait of a 3D underactuated bipedal robot. The model of the robot consists of a rigid tree structure with a torso and two identical legs with point feet[6]. Each leg includes 3 actuated DOFs: a 2 DOF hip (ball) joint with roll and pitch angles plus a 1 DOF knee joint in the sagittal plane (see Figs. 1 and 2). During the single support phase, the model has 9 DOFs with 6 actuators. In particular, the roll, pitch and yaw angles associated with the torso frame are unactuated. The kinematic and dynamic parameter values for the links are taken according to those reported in [36] for a 3D human model. The continuous-time portion of the hybrid system in (1) is constructed based on the right stance phase Lagrangian dynamics with 18 state variables. The discrete-time portion is then taken as the composition of the right-to-left impact, left stance phase, and left-to-right impact models. The impact maps assume rigid and instantaneous contact models [37]. A desired periodic gait $\mathcal{O}$ is then designed using the motion planning algorithm of [8] for walking at 0.6 (m/s) with the cost of mechanical transport CMT = 0.07.

The two-part decentralization scheme in Fig. 2 is motivated by a transpelvic amputee (the "human" part) walking with a prosthetic left leg (the "prosthetic" part). The prosthetic subsystem Σ_2 includes the 3 DOFs of the left leg with the corresponding 3 actuators and hence, $\dim(x_2) = 6$ and $\dim(u_2) = 3$. The human subsystem Σ_1 consists of the rest of the model, including the torso and right leg, with $\dim(x_1) = 12$ and $\dim(u_1) = 3$. The set of measurable global variables $\Psi_2(x)=(\psi_2^\top(x), \dot{\psi}_2^\top(x))^\top$ for subsystem Σ_2 includes two roll and yaw angles as well as their velocities provided by the two IMUs attached to the model thighs (i.e., $\dim(\psi_2) = 4$ and $\dim(\Psi_2) = 8$). Next the local output matrices to be determined then include $H_1(\xi_1) \in \mathbb{R}^{3\times 6}$, $H_2(\xi_2) \in \mathbb{R}^{3\times 3}$, and $\hat{H}_2(\xi_2) \in \mathbb{R}^{3\times 4}$, or equivalently 39 parameters[7]. However, since the typical walking period includes two steps, we need to determine these matrices for the right and left stance phases and hence, the total number of parameters is $39 \times 2 = 78$, i.e., $\xi \in \mathbb{R}^{78}$.

B. PENBMI Solver and Numerical Results

BMIs are NP-hard problems. However, available software packages like PENBMI [38] are general purpose, local solvers which guarantee the convergence to a critical point satisfying the first-order Karush-Kuhn-Tucker (KKT) conditions. An initial set of local virtual constraints with the parameter vector $\xi^0 \in \mathbb{R}^{78}$ is assumed based on physical intuition to

[6]We make use of the point foot assumption to simplify the hybrid model of walking, but the results can be applied to hybrid models of walking with nontrivial feet.

[7]We remark that $\hat{H}_1 = 0$. In addition, since the outputs in (7) need to be holonomic, we replace $x_{i,1}$ and $x_{d,i,1}(\theta)$ in (7) with the local configuration variables q_i and the corresponding desired evolution $q_{d,i}(\theta)$, respectively.

initiate the iterative algorithm. For this set of local virtual constraints, the dominant eigenvalues of the 17 ×17 Jacobian of the Poincaré map and the corresponding spectral radius become {0.1029 ±1.7223i,−0.4683,−0.4178} and 1.7253, respectively. Hence, the orbit is unstable. To stabilize the orbit, we employ the iterative BMI algorithm with the weighting factor $w = 1$. The BMI optimization problem (12)–(15) during each iteration of the algorithm is then solved with the PENBMI solver from TOMLAB [39] integrated with MATLAB environment through YALMIP [40]. The BMI optimization procedure on a computer with a dual 2.3 GHz Intel Xeon E5-2670 v3 processor takes approximately 15 minutes. The iterative algorithm successfully converges to a stabilizing set of parameters after 5 iterations. For the BMI optimized parameters, the dominant eigenvalues and spectral radius of the Poincaré map Jacobian become {0.4908,−0.0058 −0.4681i,−0.3153} and 0.4908, respectively, and hence, the desired periodic gait $\mathcal{O}$ becomes exponentially stable (71.56% decrease in the spectral radius). Figure 2 depicts the phase portraits of the BMI optimized closed-loop system. Here, the simulation starts off of the orbit at the beginning of the right stance phase with an initial error of −2 (deg/s) in the velocity components. Convergence to the periodic orbit is clear. The animation of this simulation can be found at [41].

V. CONCLUSIONS

This paper introduced an algorithm to systematically design time-invariant decentralized feedback controllers for exponential stabilization of periodic orbits for a class of hybrid dynamical systems arising from bipedal walking. The algorithm is developed based on an iterative sequence of optimization problems involving BMIs and LMIs. It can address a general form of parameterized and nonlinear local controllers in which the coordination of lower-dimensional subsystems is done by a common measurable phasing variable. The algorithm accounts for high degrees of underactuation and strong interactions among subsystems and can be solved effectively with available software packages. The numerical results illustrate the power of the algorithm in designing stabilizing local nonlinear controllers for a hybrid model of walking with 18 state variables and 78 control parameters. For future research, we will investigate the scalability of the algorithm and its capability in stabilizing larger size interconnected systems. We will also investigate the design of robust decentralized feedback solutions against uncertainties in the hybrid models.

References

1. Song, G.; Zefran, M. Underactuated dynamic three-dimensional bipedal walking. Robotics and Automation. Proceedings IEEE International Conference on; May 2006; p. 854-859.
2. Grizzle J, Abba G, Plestan F. Asymptotically stable walking for biped robots: analysis via systems with impulse effects. Automatic Control, IEEE Transactions on. Jan; 2001 46(1):51–64.
3. Westervelt E, Grizzle J, Koditschek D. Hybrid zero dynamics of planar biped walkers. Automatic Control, IEEE Transactions on. Jan; 2003 48(1):42–56.
4. Spong M, Bullo F. Controlled symmetries and passive walking. Automatic Control, IEEE Transactions on. Jul; 2005 50(7):1025–1031.
5. Spong M, Holm J, Lee D. Passivity-based control of bipedal locomotion. Robotics Automation Magazine, IEEE. Jun; 2007 14(2):30–40.
6. Ames, A.; Gregg, R.; Spong, M. A geometric approach to three-dimensional hipped bipedal robotic walking. Decision and Control, 46th IEEE Conference on; Dec 2007; p. 5123-5130.

7. Ames A. Human-inspired control of bipedal walking robots. Automatic Control, IEEE Transactions on. May; 2014 59(5):1115–1130.
8. Ramezani A, Hurst J, Akbai Hamed K, Grizzle J. Performance analysis and feedback control of ATRIAS, a three-dimensional bipedal robot. Journal of Dynamic Systems, Measurement, and Control December, ASME. Dec.2013 136(2)
9. Dai, H.; Tedrake, R. L_2-gain optimization for robust bipedal walking on unknown terrain. Robotics and Automation, IEEE International Conference; May 2013; p. 3116-3123.
10. Manchester IR, Mettin U, Iida F, Tedrake R. Stable dynamic walking over uneven terrain. 2011; 30(3):265–279.
11. Byl, K.; Tedrake, R. Approximate optimal control of the compass gait on rough terrain. Robotics and Automation. IEEE International Conference; May 2008; p. 1258-1263.
12. Song S, Geyer H. A neural circuitry that emphasizes spinal feedback generates diverse behaviours of human locomotion. The Journal of Physiology. 2015
13. Villarreal DJ, Poonawala H, Gregg RD. A robust parameterization of human gait patterns across phase-shifting perturbations. IEEE Trans Neural Systems and Rehabilitation Engineering. 2016 conditionally accepted.
14. Sup F, Varol H, Goldfarb M. Upslope walking with a powered knee and ankle prosthesis: Initial results with an amputee subject. IEEE Transactions on Neural Systems and Rehabilitation Engineering. 2011; 19(1):71–78. [PubMed: 20952344]
15. Simon AM, Ingraham KA, Fey NP, Finucane SB, Lipschutz RD, Young AJ, Hargrove LJ. Configuring a powered knee and ankle prosthesis for transfemoral amputees within five specific ambulation modes. PloS ONE. 2014; 9(6):e99387. [PubMed: 24914674]
16. Gregg R, Lenzi T, Hargrove L, Sensinger J. Virtual constraint control of a powered prosthetic leg: From simulation to experiments with transfemoral amputees. Robotics, IEEE Transactions on. Dec; 2014 30(6):1455–1471.
17. Gregg R, Sensinger J. Towards biomimetic virtual constraint control of a powered prosthetic leg. Control Systems Technology, IEEE Transactions on. Jan; 2014 22(1):246–254.
18. Martin, A.; Gregg, R. Hybrid invariance and stability of a feedback linearizing controller for powered prostheses. American Control Conference; 2015; p. 4670-4676.
19. Siljak, D. Decentralized Control of Complex Systems. Dover Publications; Dec. 2011
20. Bakule L. Decentralized control: An overview. Annual Reviews in Control. 2008; 32(1):87–98.
21. Wang S-H, Davison E. On the stabilization of decentralized control systems. Automatic Control, IEEE Transactions on. Oct; 1973 18(5):473–478.
22. Haddad, W.; Chellaboina, V.; Nersesov, S. Impulsive and Hybrid Dynamical Systems: Stability, Dissipativity, and Control. Princeton University Press; Jul. 2006
23. Goebel, R.; Sanfelice, R.; Teel, A. Hybrid Dynamical Systems: Modeling, Stability, and Robustness. Princeton University Press; Mar. 2012
24. Burden S, Revzen S, Sastry S. Model reduction near periodic orbits of hybrid dynamical systems. Automatic Control, IEEE Transactions on. 2015 to appear.
25. Akbari Hamed K, Buss B, Grizzle J. Exponentially stabilizing continuous-time controllers for periodic orbits of hybrid systems: Application to bipedal locomotion with ground height variations. The International Journal of Robotics Research. Jun.2015 accepted to appear. doi: 10.1177/0278364915593400
26. Akbari Hamed, K.; Buss, B.; Grizzle, J. Continuous-time controllers for stabilizing periodic orbits of hybrid systems: Application to an underactuated 3D bipedal robot. Decision and Control (CDC), 2014 IEEE 53rd Annual Conference; Dec 2014; p. 1507-1513.
27. Akbari Hamed, K.; Grizzle, J. Iterative robust stabilization algorithm for periodic orbits of hybrid dynamical systems: Application to bipedal running. The IFAC Conference on Analysis and Design of Hybrid Systems; October 2015; p. 161-168.
28. Stein JL, Flowers WC. Stance phase control of above-knee prostheses: Knee control versus sach foot design. J Biomech. 1987; 20(1):19–28. [PubMed: 3558425]
29. Lack, J.; Powell, M.; Ames, A. Planar multi-contact bipedal walking using hybrid zero dynamics. Robotics and Automation, IEEE International Conference on; May 2014; p. 2582-2588.

30. Chevallereau C, Abba G, Aoustin Y, Plestan F, Westervelt E, Canudas-de Wit C, Grizzle J. RABBIT: a testbed for advanced control theory. Control Systems Magazine, IEEE. Oct; 2003 23(5):57–79.
31. Sreenath K, Park H-W, Poulakakis I, Grizzle J. Embedding active force control within the compliant hybrid zero dynamics to achieve stable, fast running on mabel. 2013; 32(3):324–345.
32. Maggiore M, Consolini L. Virtual holonomic constraints for Euler Lagrange systems. Automatic Control, IEEE Transactions on. Apr; 2013 58(4):1001–1008.
33. Shiriaev, A.; Sandberg, A.; Canudas de Wit, C. Motion planning and feedback stabilization of periodic orbits for an acrobot. Decision and Control. 43rd IEEE Conference on; Dec 2004; p. 290-295.
34. Sreenath K, Park H-W, Poulakakis I, Grizzle JW. Compliant hybrid zero dynamics controller for achieving stable, efficient and fast bipedal walking on MABEL. The International Journal of Robotics Research. Aug; 2011 30(9):1170–1193.
35. Martin AE, Post DC, Schmiedeler JP. The effects of foot geometric properties on the gait of planar bipeds walking under HZD-based control. 2014; 33(12):1530–1543.
36. de Leva P. Adjustments to Zatsiorsky-Seluyanov's segment inertia parameters. J Biomech. 1996; 29(9):123–1230. [PubMed: 8839025]
37. Hurmuzlu Y, Marghitu DB. Rigid body collisions of planar kinematic chains with multiple contact points. 1994; 13(1):82–92.
38. Henrion, D.; Lofberg, J.; Kocvara, M.; Stingl, M. Solving polynomial static output feedback problems with PENBMI. Decision and Control, and European Control Conference. 44th IEEE Conference on; Dec 2005; p. 7581-7586.
39. TOMLAB optimization. http://tomopt.com/tomlab/
40. Lofberg, J. YALMIP : a toolbox for modeling and optimization in MATLAB. Computer Aided Control Systems Design, 2004 IEEE International Symposium on; Sept 2004; p. 284-289.
41. K Akbari Hamed YouTube Channel. Decentralized feedback controllers for stabilization of hybrid periodic orbits. 2015. https://www.youtube.com/watch?v=WuUfS_7SalQ

APPENDIX

Proof of Lemma 1

For a given matrix A, $\rho(A) < \gamma$ for some positive γ is equivalent to matrix $\frac{1}{\gamma}A$ being Hurwitz. This is equivalent to the existence of $Y = Y^\top > 0$ such that $\frac{1}{\gamma^2}A^\top YA - Y < 0$. Pre and post multiplying this latter inequality by $W = Y^{-1} > 0$ and employing Schur's complement Lemma results in $[WAW; \star\ \gamma^2 W] > 0$. Finally choosing $\gamma^2 := 1-\mu < 1$ in the BMI problem (12)–(15) together with $\eta > \|\Delta\xi^\ell\|_2^2$ from the LMI (14) completes the proof.

Proof of Theorem 1

For the scalar case, $\rho(\tilde{a}(\xi^\ell, \Delta\xi^\ell)) < \gamma$ is equivalent to $|\tilde{a}(\xi^\ell, \Delta\xi^\ell)| = |a(\xi^\ell) + a'(\xi^\ell)\Delta\xi^\ell| < \gamma$. Using this fact, the Lagrange multipliers and assumption (20), it can be shown that the global optimal solution of (17)–(19) is given by $\Delta\xi^{\ell\star} = -\frac{w\, a^\ell\, a'^\ell}{w(a'^\ell)^2+1}$, where $a^\ell := a(\xi^\ell)$ and $a'^\ell := a'(\xi^\ell)$. This results in the parameter update law $\xi^{\ell+1} = \xi^\ell - \frac{w\, a^\ell\, a'^\ell}{w(a'^\ell)^2+1} =: Q(\xi^\ell)$ with an equilibrium point at $\xi = \bar{\xi}$. It can also be shown that under assumption $a'(\xi) \neq 0$ for $\xi \in \mathbb{R}$, $0 < \frac{\partial Q}{\partial \xi}(\bar{\xi}) = \frac{1}{w(a'(\bar{\xi}))^2+1} < 1$ and hence, the equilibrium point $\bar{\xi}$ is exponentially stable. This implies the existence of $\delta > 0$ such that for all $\xi^0 \in \mathbb{R}$ with the property $|\xi^0 - \bar{\xi}| < \delta$, $\lim_{\ell\to\infty}$

$\xi^\ell = \bar{\xi}$. Furthermore, $|\xi^\ell - \bar{\xi}| \leq |\xi^0 - \bar{\xi}| < \delta$ for $\ell = 0, 1, \cdots$ which follows that $\xi^\ell \in \mathcal{B}$ for $\ell = 0, 1, \cdots$. Finally, since $a(\xi)$ is smooth, $\lim_{\ell\to\infty} a(\xi^\ell) = a(\lim_{\ell\to\infty} \xi^\ell) = a(\bar{\xi}) = 0$ which implies that there is $N > 0$ such that for all $\ell > N$, $|a(\xi^\ell)| < 1$.

Proof of Theorem 2

The proof is similar to that presented in [27, Theorem 2]. During iteration ℓ, we define an *error function* $E(\Delta\xi) \in \mathbb{R}^{n+1}$ with the components

$$E_\alpha(\Delta\xi) := F_\alpha\left(a\left(\xi^\ell + \Delta\xi\right), \gamma^\ell\right) - F_\alpha\left(\hat{a}\left(\xi^\ell, \Delta\xi\right), \gamma^\ell\right)$$

for $\alpha = 1, \cdots, n+1$, where $\gamma^\ell := \sqrt{1-\mu^{\ell\star}}$. This function satisfies $E(0) = 0$ and $\frac{\partial E}{\partial \Delta\xi}(0) = 0$. The conditions (22) imply that $\frac{\partial^2 E_\alpha}{\partial \Delta\xi^2}(0) \leq 0$ for $\alpha = 1, \cdots, n+1$ which are second-order optimality conditions under which the components of E reach a local maximum at $\Delta\xi = 0$. Hence, for $\|\Delta\xi^{\ell\star}\| < \varepsilon$, $E_\alpha(\Delta\xi^{\ell\star}) \leq E_\alpha(0) = 0$ or $F_\alpha(a(\xi^\ell + \Delta\xi^{\ell\star}), \gamma^\ell) \leq F_\alpha(\hat{a}(\xi^\ell, \Delta\xi^{\ell\star}), \gamma^\ell) < 0$ for $\alpha = 1, \cdots, n+1$. Hence, $\rho(A(\xi^\ell + \Delta\xi^{\ell\star})) < \gamma^\ell$. Finally, from the feasibility assumption of the BMI problem and the equivalent problem in Lemma 1, $\gamma^\ell = \sqrt{1-\mu^{\ell\star}} < 1$.

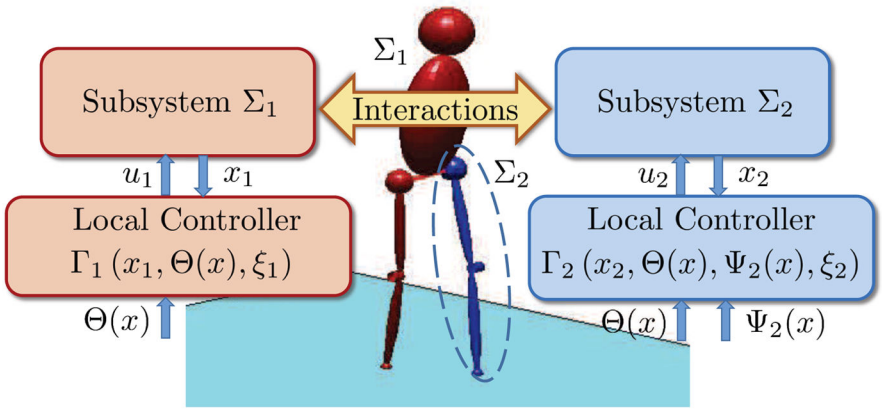

Fig. 1.

Illustration of the local subsystems and proposed decentralized feedback control scheme for stabilization of hybrid periodic orbits for bipedal walking. The subsystem Σ_2 (i.e., prosthetic part), shown by the dashed ellipse, includes the degrees of freedom and actuators for the left leg. Σ_1 (i.e., human part) consists of the rest of the model.

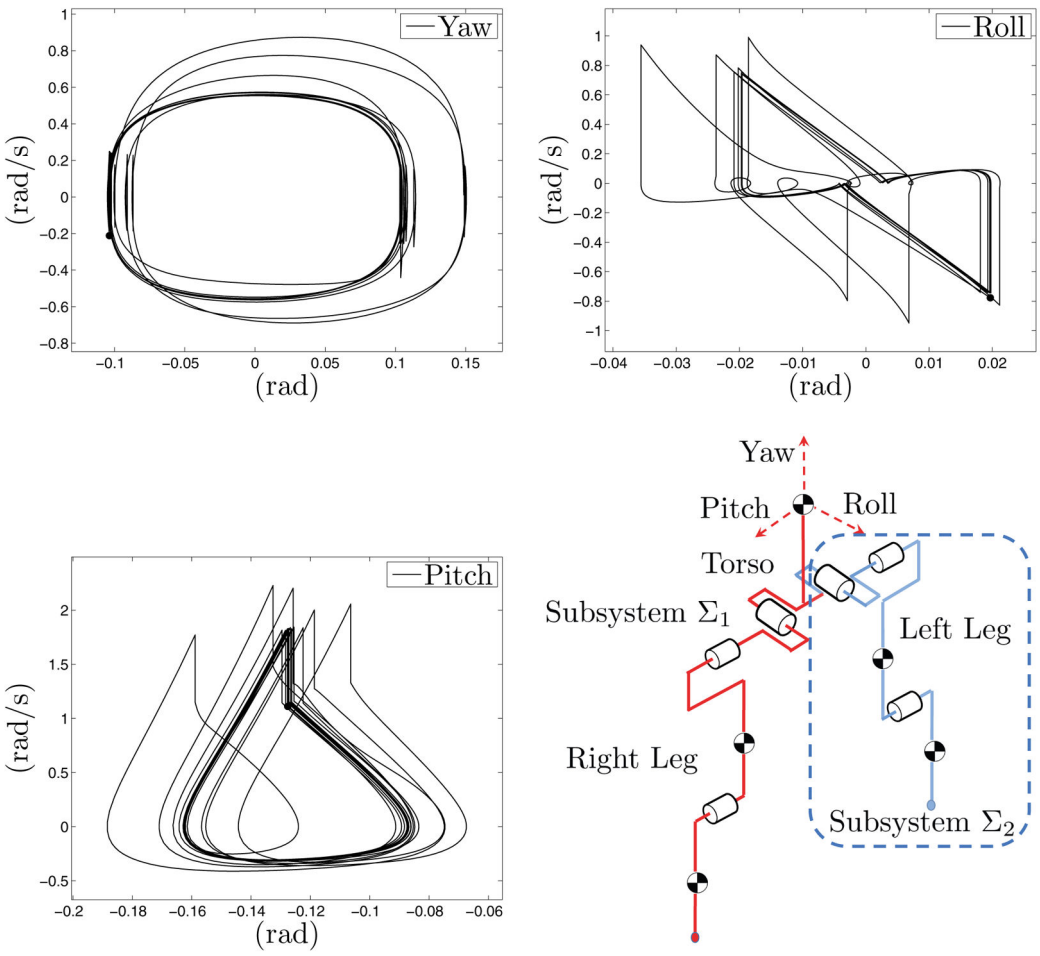

Fig. 2.

Phase portraits for the torso Euler angles (yaw, roll and pitch) during 50 consecutive steps of 3D walking by the BMI optimized decentralized feedback control scheme together with the structure of the 9 DOFs autonomous bipedal robot. The model consists of three unactuated Euler angles and 6 actuated revolute joints. Subsystems Σ_1 and Σ_2 with the corresponding DOFs have been shown in the figure.